9. D. Geer, UWB standardization effort ends in controversy, Computer 39 (2006), 13–16.
10. W. Hirt, The European UWB radio regulatory and standards framework: Overview and implications, IEEE International Conference on Ultra-Wideband, ICUWB 2007, pp.733–738, 24–26.
11. A. Giorgetti, M. Chiani, D. Dardari, R. Piesiewicz, and G.H. Bruck, The cognitive radio paradigm for ultra-wideband systems: The European project EUWB, IEEE International Conference on Ultra-Wideband, ICUWB 2008, Vol. 2, pp.169–172, 10–12.
12. M. Karlsson and S. Gong, Circular dipole antenna for Mode 1 UWB radio with integrated balun utilizing a flex-rigid structure, IEEE Trans Antennas Propag 57 (2009), 2967–2971.
13. S. Chakraborty, N.R. Belk, A. Batra, M. Goel, and A. Dabak, Towards fully integrated wideband transceivers: fundamental challenges, solutions and future, Proc. IEEE Radio-Frequency Integration Technology: Integrated Circuits for Wideband Communication and Wireless Sensor Networks 2005, pp. 26–29.
14. H. Schantz, The art and science of ultrawideband antennas, Artech House Inc., Norwood, MA, 2005.
15. M. Karlsson, P. Håkansson, A. Huynh, and S. Gong, Frequency-multiplexed inverted-F antennas for multi-band UWB, IEEE Wireless Microwave Conf. 2006, pp. 2.1–2.3.
16. Z.N. Chen, M.J. Ammann, X. Qing; X.H. Wu, T.S.P. See, and A. Cai, Planar antennas, IEEE Microwave Mag 7 (2006), 63–73.
17. W.S. Lee, D.Z. Kim, K.J. Kim, K.S. Son, W.G. Lim, and J.W. Yu, Multiple frequency notched planar monopole antenna for multi-band wireless systems, Proc. IEEE 35th European Microwave Conf., Paris, France, 2005, pp. 535–537.
18. X.H. Wu and Z.N. Chen, Comparison of planar dipoles in UWB applications, IEEE Trans Antennas Propag 53 (2005) 1973–1983.
19. T.-G. Ma and S.-K. Jeng, A printed dipole antenna with tapered slot feed for ultrawide-band applications, IEEE Trans Antennas Propag 53 (2005) 3833–3836.
20. R. Bourtoutian, C. Delaveaud, and S. Toutain, Differential, Shorted Dipole Antenna for European UWB Applications, The Second European Conference on Antennas and Propagation, EuCAP 2007, pp. 1–5.
21. J.-P. Zhang, Y.-S. Xu, and W.-D. Wang, Microstrip-fed semi-elliptical dipole antennas for ultrawideband communications, IEEE Trans Antennas Propag 56 (2008), 241–244.
22. C.-D. Zhao, Analysis on the properties of a coupled planar dipole UWB antenna, IEEE Antennas and Wireless Propag Lett 3 (2004), 317–320.
23. B. Kim, S. Nikolaou, G.E. Ponchak, Y.-S. Kim, J. Papapolymerou, and M.M. Tentzeris, A curvature CPW-fed ultra-wideband monopole antenna on liquid crystal polymer substrate using flexible characteristic, IEEE Antennas and Propagation Society Int. Symp., Albuquerque, NM, 2006, pp. 1667–1670, 9–14.
24. J.S. McLean, H. Foltz, and R. Sutton, Pattern descriptors for UWB antennas, IEEE Trans Antennas Propag 53 (2005), 553–559.
25. J. McLean, H. Foltz, and R. Sutton, Conditions for direction-independent distortion in UWB Antennas, IEEE Trans Antennas Propag 54 (2006), 3178–3183.
26. T. Dissanayake and K.P. Esselle, Prediction of the notch frequency of slot loaded printed UWB antennas, IEEE Trans Antennas Propag 55 (2007), 3320–3325.
27. D. Valderas, R. Alvarez, J. Melendez, I. Gurutzeaga, J. Legarda, and J.I. Sancho, UWB staircase-profile printed monopole design, IEEE Antennas Wirel Propag Lett 7 (2008), 255–259.
28. M.E. Bialkowski and A.M. Abbosh, Design of UWB planar antenna with improved cut-off at the out-of-band frequencies, IEEE Antennas Wirel Propag Lett 7 (2008), 408–410.
29. W. Wiesbeck, G. Adamiuk, and C. Sturm, Basic properties and design principles of UWB antennas, Proc IEEE 97 (2009), 372–385.
30. J.R. Costa, C.R. Medeiros, and C.A. Fernandes, Performance of a crossed exponentially tapered slot antenna for UWB systems, IEEE Trans Antennas Propag 57 (2009), 1345–1352.
31. Y. Duroc, A.I. Najam, T.P. Vuong, and S. Tedjini, Modeling and state representation of ultrawideband antennas, IEEE Trans Antennas Propag 57 (2009), 2781–2784.
32. B.S. Yildirim, B.A. Cetiner, G. Roqueta, and L. Jofre, Integrated bluetooth and UWB antenna, IEEE Antennas Wirel Propag Lett 8 (2009), 149–152.
33. K.S. Ryu and A.A. Kishk, UWB antenna with single or dual band-notches for lower WLAN band and upper WLAN band, IEEE Trans Antennas Propag 57 (2009), 3942–3950.
34. V.F. Fusco, Foundations of antenna theory and techniques, Pearson Education Limited, Edinburgh Gate, Harlow, Essex, England, 2005, p. 45.
35. M. Karlsson, P. Hakansson, and S. Gong, A frequency triplexer for ultra-wideband systems utilizing combined broadside- and edge-coupled filters, IEEE Trans Adv Pack 31 (2008), 794–801.

HIGH SELECTIVITY MINIATURIZED BROADBAND FILTER

D. Packiaraj,[1] K. J. Vinoy,[2] M. Ramesh,[1] and A. T. Kalghatgi[1]
[1] Central Research Laboratory, Bharat Electronics Limited, Bangalore - 560 013, India; Corresponding author: dpackiaraj@bel.co.in
[2] Department of Electrical Communication Engineering, Indian Institute of Science, Bangalore - 560 012, India

Received 29 March 2010

ABSTRACT: *Design of a compact broadband filter using tightly coupled line sections in defected (A slot is cut in the ground) microstrip medium operating from 3.1–6.8 GHz has been reported in this article. Filter has been designed and analyzed using an equivalent circuit model based on even and odd mode parameters of coupled line sections. The proposed filter has attenuation poles on either side of the pass band resulting in improved selectivity. This filter features spurious-free response up to third harmonic frequency. Experimental results of the filter have been validated against the analytical and full wave simulations.* © 2010 Wiley Periodicals, Inc. Microwave Opt Technol Lett 53:184–187, 2011; View this article online at wileyonlinelibrary.com. DOI 10.1002/mop.25676

Key words: *broadband; coupled line; filter; slot*

1. INTRODUCTION

Compact broadband miniature filters find applications in various wireless communication systems such as electronic warfare, ultra wide band (UWB), etc. Multi-band offset frequency division modulation (MB-OFDM) UWB is gaining popularity due to its low power and high data rate features. In the MB-OFDM approach, the complete frequency band (3.1–10.6 GHz) has been divided into 14 bands (five groups) with each band occupying 528 MHz bandwidth. In MB-OFDM, two UWB devices communicate using adjacent frequency bands. Broadband filter with high selectivity is one of the key elements in such systems. This article presents the design of a compact broadband filter suitable for MB-OFDM UWB devices operating over 3.1–6.8 GHz, three adjacent band groups of FCC designated UWB frequency band.

Most of the filters in reported literature [1–5] use half wave or quarter wave coupled resonators, defected ground based structures, stepped impedances, and multi-mode resonators to realize wideband filter. Wide band filters using metallization on both sides of suspended stripline substrate are realized in [6]. Metallization on multi-layers provide tight coupling between lines to achieve wide bandwidth. In [7], a ''Y'' shaped dual mode microstrip wide bandpass filter with input-output cross coupling is designed and implemented. Broadside coupled lines

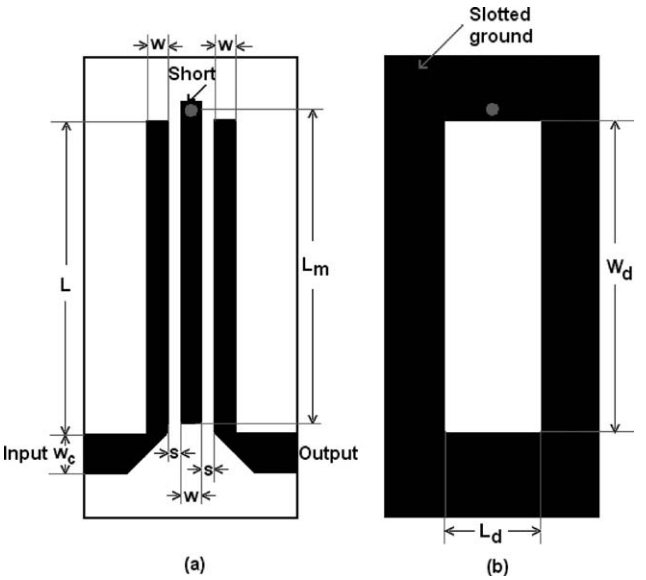

Figure 1 Proposed broadband filter. (a) Top layer and (b) bottom layer

with spur lines are used for designing UWB filter in [8] with improved stop band rejection characteristics.

In this article, a new configuration of compact broadband filter realized in defected microstrip medium is presented. As shown in Figure 1, this filter consists of coupled quarter wave resonators above a slotted ground with a short circuited middle resonator. This filter can be treated as modification to the one reported in [7] with an open circuited middle half wave resonator replaced by a short circuited quarter wave resonator to improve the spurious suppression. Further slotted ground has been used to enhance the bandwidth of the filter. Shorted quarter wave resonator is used to suppress the spurious at the second harmonic frequency.

The article is organized as follows. Analysis of the filter based on circuit model using even and odd mode parameters is explained in Section 2. Results obtained from analytical calculations performed in MATLAB are compared against the planar simulation results from commercially available simulator IE3D from Zeland [9]. In Section 3, experimental results of measured broadband filter are compared against the simulation results. Section 4 concludes this article.

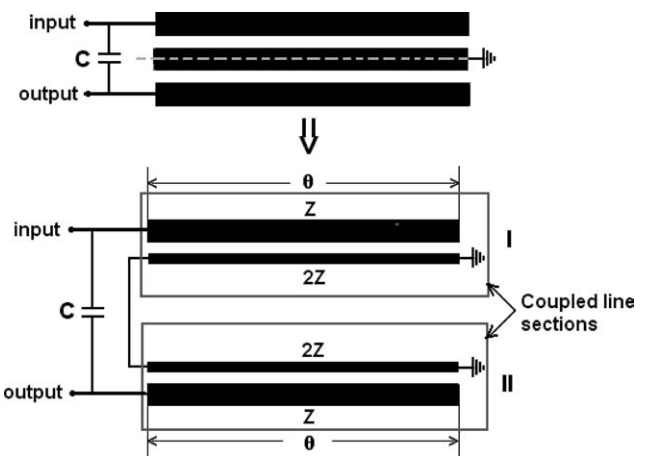

Figure 2 The filter and its coupled line sections

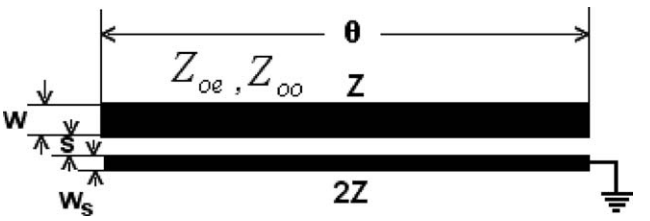

Figure 3 Coupled line section

2. ANALYSIS OF BROADBAND FILTER

The proposed filter is designed from 3.1 to 6.8 GHz (75% fractional bandwidth) and is implemented in a microstrip medium having a substrate thickness "h" of 0.787 mm and permittivity "ε_r" of 2.17. The top layer of the filter has input and output feed lines coupled to a short circuited quarter wave resonator. The bottom layer has slotted ground. The slot in the ground plane enhances the coupling to widen the pass band of the filter. The filter has attenuation poles on either side of the pass band. The cross coupling between the input and output generates the attenuation poles at the lower and upper stop bands. This filter exhibits spurious-free response up to the third harmonic frequency due to the short circuited resonator.

2.1. Analysis

The entire filter can be viewed as formed from two identical asymmetrical coupled sections as shown in Figure 2. The coupled line section is shown in Figure 3. "C" is cross coupling capacitor between input and output feed lines.

Coupled line sections can be characterized using impedance "Z" parameters given by [1]

$$Z_{11} = -j(Z_{oe} + Z_{oo})\frac{\cot\theta}{2} + j\frac{(Z_{oe} - Z_{oo})^2}{Z_{oe} + Z_{oo}}\csc 2\theta \quad (1a)$$

$$Z_{12} = Z_{21} = j(Z_{oe} - Z_{oo})\frac{\tan\ \theta}{2} \quad (1b)$$

$$Z_{22} = j(Z_{oe} + Z_{oo})\frac{\tan\ \theta}{2} \quad (1c)$$

$$\theta = \sqrt{\theta_e\theta_o} \quad (2)$$

where Z_{oe} and Z_{oo} are even and odd mode impedances, respectively. θ_e and θ_o are even and odd mode phase velocities, respectively.

TABLE 1 Physical Parameters of Filter

Parameters	Values
Width of feed line (w_c)	2.4 mm
Width of coupled line (w)	0.5 mm
Width of coupled line (w_s)	0.04 mm
Spacing (s)	0.2 mm
Length of coupled lines (L, L_m)	(11,11.7) mm
Size of slot on the ground (L_d, W_d)	(1.9, 11) mm

TABLE 2 Electrical Parameters of Filter

Parameters	Values
Even and odd mode impedances (Z_{oe}, Z_{oo}) of coupled lines Sections 1, 2	(220,100) Ω
Electrical length (θ) at the center frequency	90°
Cross coupling capacitor (C)	0.005 pF
Line impedance (Z)	145 Ω
Input and output impedances	50 Ω

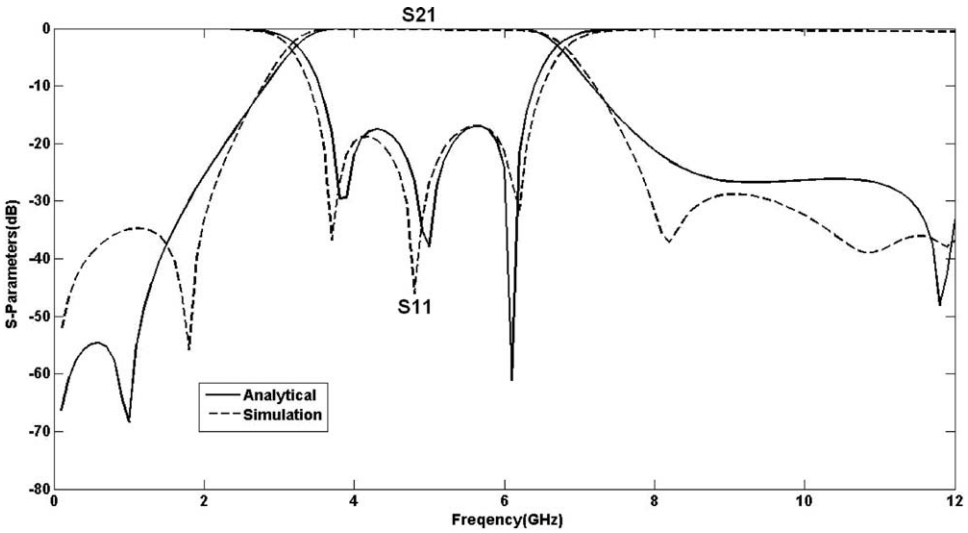

Figure 4 Analytical results of broadband filter

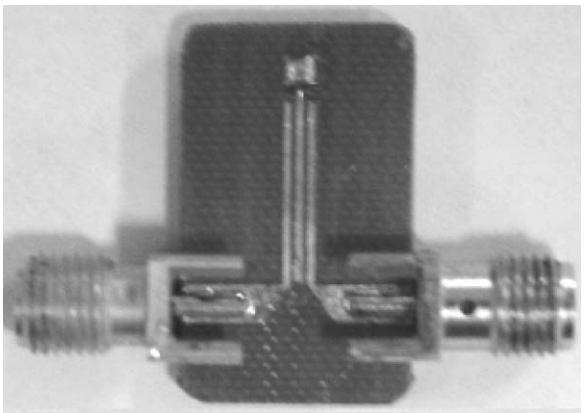

Figure 5 Photograph of broadband filter

2.2. Design

Filter is designed with the following specifications

- Frequency band: 3.1–6.8 GHz
- Substrate thickness "h": 0.78 mm
- Substrate permittivity "ε_r": 2.17.

Physical and corresponding electrical parameters of the filter are given in Tables 1 and 2, respectively. Z_{oe} and Z_{oo} are even and odd mode impedances of coupled lines (with defected ground) having widths of "w" and "w_s" and gap "s". The length of coupled line section is quarter wavelength at the center frequency (4.95 GHz) of the filter. Transmission matrices of coupled line Sections 1 and 2 are calculated using the impedance matrices given in Eqs. (1)–(2). Calculated transmission matrices of coupled line sections and cross coupling capacitor are used to calculate the scattering parameters. Figure 4 shows the comparison between analytical results and full wave simulation results [9] and a close agreement between them can be observed.

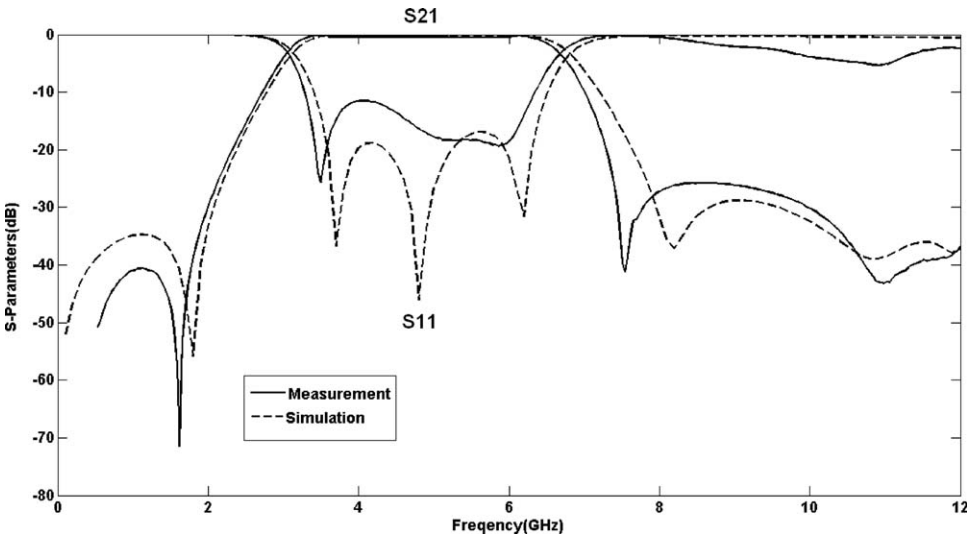

Figure 6 Measured results of broadband filter

3. EXPERIMENTAL RESULTS

The filter is machined using LPKF printed circuit board prototyping machine. Figure 5 shows the photograph of the experimental broadband filter. Figure 6 compares the experimental results of designed filter against the full wave simulation results. Comparison shows a good agreement between them confirming the expected broadband and suppressed second harmonic features. Frequency band of the filter is 3.1 to 6.75 GHz. Maximum insertion loss of the filter is 0.4 dB, and return loss is better than 13 dB. Stop band rejection is better than 25 dB over 7.5 GHz to 12 GHz while the second harmonic (9.9 GHz) of the filter has been suppressed to a level of 30 dB. Filter is compact and size is $12 \times 15 \times 0.78$ mm^3.

4. CONCLUSION

Using a quarter wave coupled microstrip resonator in a defected ground configuration, a broadband filter from 3.1–6.8 GHz was designed and analyzed. Filter used a short circuited quarter wave resonator for second harmonic suppression. The filter exhibited 0.4 dB insertion loss and 13 dB return loss over the pass band. The results of analysis were confirmed through experiment. Overall dimensions of the filter are $12 \times 15 \times 0.78$ mm^3.

REFERENCES

1. G. Matthaei, L. Young, and E.M.T. Jones, Microwave filters, impedance matching networks and coupling structures, reprint ed., Artech House Inc, Norwood, MA, 1985.
2. D. Packiaraj, K.J. Vinoy, and A.T. Kalghatgi, Analysis and design of a compact multi-layer ultra wide band filter, Prog Electromagn Res C 7 (2009), 111–123.
3. C.H. Liang and C.Y. Chang, Compact wideband bandpass filters using stepped-impedance resonators and interdigital coupling structures, IEEE Microwave Wireless Compon Lett 19 (2009), 551–553.
4. C.Y. Hsu, C.Y. Chen, and C.H. Huang, A UWB filter using a dual-mode ring resonator with spurious pass band suppression, Microwave J 48 (2005), 130–136.
5. L. Zhu, S. Sun, and W. Menzel, Ultra-wideband (UWB) bandpass filters using multiple-mode resonator, IEEE Microwave Wireless Compon Lett 15 (2005), 796–798.
6. W. Schwab, F. Boegelsack, and W. Menzel, Multilayer suspended stripline and coplanar line filters, IEEE Trans Microwave Theory Technol 42 (1994), 1403–1407.
7. L. Zhu, S. Sun, and W. Menzel, Novel broadband bandpass filters using y-shaped dual-mode microstrip resonators, IEEE Microwave Wireless Compon Lett 19 (2009), 548–550.
8. D. Packiaraj, K.J. Vinoy, and A.T. Kalghatgi, Analysis and design of two layered ultra wide band filter, J Electromagn Waves Appl 23 (2009), 1235–1243.
9. Zeland Software Inc., IE3D 11.5, Fremont, CA, 2006.

MULTIOCTAVE MICROSTRIP-TO-COPLANAR WAVEGUIDE VERTICAL TRANSITION

A. M. Abbosh
School of ITEE, The University of Queensland, Qld. 4072, Australia; Corresponding author: a.abbosh@uq.edu.au

Received 29 March 2010

ABSTRACT: *A vialess vertical microstrip-to-coplanar waveguide (CPW) transition that covers a multioctave bandwidth is proposed. The proposed transition utilizes the magnetic coupling in a pair of mcirostrip-to-slotline transitions derived from the microstrip/CPW structure. The presented device is designed following simple design guidelines. The simulated and measured results show that the proposed transition can achieve a six-octave bandwidth.* © 2010 Wiley Periodicals, Inc. Microwave Opt Technol Lett 53:187–189, 2011; View this article online at wileyonlinelibrary.com. DOI 10.1002/mop.25675

Key words: *transition; coplanar waveguide; microstrip*

1. INTRODUCTION

As microwave circuits become more compact, new techniques for integration are being utilized. In the modern multilayer technology, the third dimension is utilized for vertical integration to reduce total space and cost. Vertical transitions are thus crucial in the design of multilayer circuits.

Microwave circuits are usually based on planar technologies, such as microstrips and/or coplanar waveguides (CPW), as they provide a compact, lightweight, and low-loss transmission medium. Concerning the multilayer integrated circuits, they require a flexibility to use both microstrip and CPW circuit technologies [1]. Therefore, vertical transitions between microstrip and CPW lines located at different layers are a must to accomplish the much needed flexibility in the design of multilayer circuits. In addition to that, vertical transitions can be used to develop new devices and/or to improve the performance of some of the existing devices [2, 3].

Microstrip-to-CPW vertical transitions are usually designed using either aperture-coupled structures or via-holes. Concerning the via-hole transitions, it was revealed that as the operating frequency increases, the performance of the via-holes is degraded [4]. In addition, their fabrication process is usually difficult and costly as sophisticated tools are needed to minimize their additional losses [5, 6]. To overcome the shortcomings of the via-holes, aperture-coupled vertical transitions can be used [7, 8]. However, the relatively high insertion loss due to the use of compact aperture-coupled transitions in broadband applications, such as the ultra-wideband technology (3.1–10.6 GHz), is still a problem which needs to be solved.

In this article, a microstrip-to-CPW vertical transition is designed by utilizing the magnetic coupling between two 100-Ω slotlines derived from the 50-Ω CPW at the bottom layer and two 100-Ω mictrostrip lines formed by splitting the 50-Ω microstrip at the top layer. The design is accomplished following simple design guidelines. The success of the proposed transition is demonstrated via simulations and measurements.

2. DESIGN

The configuration of the proposed vertical transition is shown in Figure 1. In this configuration, the microstrip feeder is assumed to be at the top layer, while the CPW is located at the bottom layer.

The 50-Ω microstrip line is divided into two similar sections each having an impedance of 100 Ω, see Figure 1(a). Similarly, the central strip of the CPW at the bottom layer is increased in width so that it forms two slotlines extending in different directions as depicted in Figure 1(b). Thus, the microstrip-to-CPW transition is transformed into a pair of microstrip-to-slotline transitions. In each pair, the microstrip and slotline extend normally beyond each other by a distance of $\lambda/4$, where λ is the effective wavelength calculated at the center of the frequency band. This configuration can be considered a magnetic-coupled structure. A signal flowing into each of the microstrip lines projects a strong magnetic field through one of the slotline opening at the other side of the substrate, and thus, it enables the normal slotline propagating mode. Therefore, the signal is efficiently